

Orientation-dependent biases in length judgments of isolated stimuli

Jielei Emma Zhu

Center for Neural Science and Department of Psychology, New York University, New York, NY, USA



Wei Ji Ma

Center for Neural Science and Department of Psychology, New York University, New York, NY, USA



Vertical line segments tend to be perceived as longer than horizontal ones of the same length, but this may in part be due to configuration effects. To minimize such effects, we used isolated line segments in a two-interval, forced choice paradigm, not limiting ourselves to horizontal and vertical. We fitted psychometric curves using a Bayesian method that assumes that, for a given subject, the lapse rate is the same across all conditions. The closer a line segment's orientation was to vertical, the longer it was perceived to be. Moreover, subjects tended to report the standard line (in the second interval) as longer. The data were well described by a model that contains both an orientation-dependent and an interval-dependent multiplicative bias. Using this model, we estimated that a vertical line was on average perceived as $9.2\% \pm 2.1\%$ longer than a horizontal line, and a second-interval line was on average perceived as $2.4\% \pm 0.9\%$ longer than a first-interval line. Moving from a descriptive to an explanatory model, we hypothesized that anisotropy in the polar angle of lines in three dimensions underlies the horizontal–vertical illusion, specifically, that line segments more often have a polar angle of 90° (corresponding to the ground plane) than any other polar angle. This model qualitatively accounts not only for the empirical relationship between projected length and projected orientation that predicts the horizontal–vertical illusion, but also for the empirical distribution of projected orientation in photographs of natural scenes and for paradoxical results reported earlier for slanted surfaces.

Introduction

The horizontal–vertical illusion (HVI) is the effect that a vertical line is perceived as longer than a horizontal line of the same length. This illusion may have been first described by Fick in 1851 and first studied systematically by Wilhelm Wundt in 1862. The

classic form of the illusion uses an “L” shape, and the lengths of the legs of the L are compared (Figure 1A). The HVI has been observed in both two-alternative, forced choice designs (Avery & Day, 1969; Craven, 1993; Mamassian & de Montalembert, 2010; Wolfe, Maloney, & Tam, 2005) and in continuous adjustment designs (Brosvic & Cohen, 1988; Cormack & Cormack, 1974; Hamburger & Hansen, 2010; Higashiyama, 1996; Künnapas, 1955, 1957b, 1959; Lipshits, McIntyre, Zaoui, Gurfinkel, & Berthoz, 2001; Pollock & Chapanis, 1952; Prinzmetal & Gettleman, 1993). Not only vertical lines, but also lines of other nonhorizontal orientations are perceived as longer than horizontal lines of the same length (Cormack & Cormack, 1974; Craven, 1993; Pollock & Chapanis, 1952). The HVI also occurs when the observer provides a haptic-only response (Gentaz & Hatwell, 2004; Heller, Calcaterra, Burson, & Green, 1997; Heller & Joyner, 1993) and has been observed across cultures (Jahoda & Stacey, 1970; Segall, Campbell, & Herskovits, 1963). The strength of the illusion is affected by the shape of the visual field (Künnapas, 1957b, 1959; Pearce & Matin, 1969; Prinzmetal & Gettleman, 1993; Williams & Enns, 1996), the presence of a depth or slant cue (Girgus & Coren, 1975; Gregory, 1974; Schiffman & Thompson, 1975; Von Collani, 1985; Williams & Enns, 1996), stimulus context (Armstrong & Marks, 1997), body orientation (Klein, Li, & Durgin, 2016), and whether you stand on top of a building (Jackson & Cormack, 2008).

Another factor affecting the strength of the HVI is the configuration of the line segments, in particular, whether one of the segments bisects the other (Brosvic & Cohen, 1988; Cormack & Cormack, 1974; Finger & Spelt, 1947; Girgus & Coren, 1975; Künnapas, 1955; Mamassian & de Montalembert, 2010). One study estimated the relative contributions of the “pure” HVI and the bisection illusion using a model (Mamassian &

Citation: Zhu, J. E., & Ma, W. J. (2017). Orientation-dependent biases in length judgments of isolated stimuli. *Journal of Vision*, 17(2):20, 1–19, doi:10.1167/17.2.20.

doi: 10.1167/17.2.20

Received September 5, 2016; published February 28, 2017

ISSN 1534-7362 Copyright 2017 The Authors



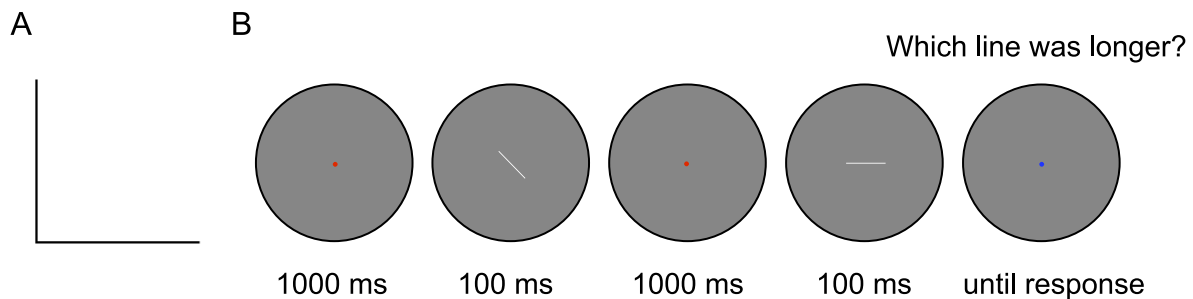


Figure 1. (A) Classic configuration used for studying the HVI (e.g., Künnapas, 1955). The vertical and horizontal line segments intersect at the bottom left corner, forming an “L” shape. The segments are equally long, but you may perceive the vertical segment to be longer. (B) Trial procedure in the present study. The subject viewed a line of variable length (the comparison line) through a circular aperture, followed by a delay period, followed by a line of fixed length (3 cm, the standard line). We varied the orientations of both lines. The subject reported which line appeared longer.

de Montalembert, 2010), but this method was indirect. Some studies presented the lines in separate intervals (Armstrong & Marks, 1997; Teghtsoonian, 1972), but these studies did not vary orientation beyond horizontal and vertical.

Here, we characterize the “pure” HVI using a two-interval design without limiting ourselves to horizontal and vertical orientations. We optimized stimulus design using a Bayesian adaptive method, which allows for precise estimation of parameters with relatively few trials. We introduce two models. The first model is descriptive: Bias is multiplicative and consists of one factor that depends on the stimulus interval and one that depends on orientation. The second model attempts to be explanatory: We show that orientation-dependent length biases can arise from anisotropy in the 3-D distribution of orientation alone.

Data and code sharing

We made all data and code publicly available on <https://github.com/EmZhu/Horizontal-Vertical-Illusion>.

Methods

Subjects

Nine subjects (four male, five female) participated in this experiment. All subjects had normal or corrected-to-normal vision as tested using a Snellen eye chart. Subjects with corrected-to-normal vision wore contact lenses, not spectacles, because they also had to wear an eye patch. Subjects gave written informed consent and received \$70 for completing the whole experiment. The study adhered to the Declaration of Helsinki and was

approved by the Institutional Review Board of New York University.

Apparatus

Subjects viewed the stimuli on a display of 2048 by 1536 pixels with a resolution of 104 pixels per centimeter and a refresh rate of 60 Hz. This display (LG LP097QX1-SPA2) was the same as that used in the 2013 iPad Air (Apple). We chose this display for its high pixel density, which reduces aliasing of oblique lines. The screen was attached to an arm of adjustable height, which was mounted on a rail. A chin rest was mounted on the same rail and adjusted such that the subject’s viewing eye was looking straight at the center of the screen. The distance between the display and eye was 44 cm, which implies that 1 cm on the screen corresponds to approximately 1.30° of visual angle.

In order to minimize external cues that could cause length biases, we took three measures: (a) We determined eye dominance using the Miles test. Subjects wore a black eye patch covering their nondominant eye. This minimizes effects due to the anisotropy of the visual field (Michaels, 1960; Prinzmetal & Gettleman, 1993). (b) We used a large piece of black cardboard with a disc (12 cm in diameter) cut out. The center of the disc was aligned with the center of the screen. The cardboard blocked out visual elements that could serve as references, such as the edges of the screen, the edges of the table, and the edges of the wall. (c) There were no light sources in the room except for the display.

Stimuli

Stimuli consisted of white line segments (luminance value: 250 out of 255) on a medium gray background

(luminance value: 128). The maximum luminance (corresponding to 255) was 390 cd/m^2 . For brevity, we refer to line segments simply as lines. The midpoint of each line was at the center of the screen. Lines were 2 pixels (0.2 mm) wide. The standard line was always 3 cm long. The length of the comparison line could take values between 2 cm and 4 cm in 61 equal steps (equal apart from rounding to an integer number of pixels). Line orientations were 0° (horizontal), 30° , 45° , 60° , 90° (vertical), 120° , 135° , and 150° . The fixation dot was 7 pixels (0.7 mm) in diameter. All stimuli were created using Psychophysics Toolbox extensions (Brainard, 1997; Pelli, 1997) in MATLAB (The MathWorks, Natick, MA). For antialiasing, we set the smoothing option of “Screen(‘DrawLines’)” to 2, which is “high-quality smoothing.” For Screen(‘BlendFunction’), we chose the most common alpha-blending factors ‘GL_SRC_ALPHA’ (source) and ‘GL_ONE_MINUS_SRC_ALPHA’ (destination).

Procedure (Figure 1B)

Trial

Each trial started with a red fixation dot in the center of the screen (1000 ms), followed by a display of the comparison line (100 ms), another screen with a red fixation dot (1000 ms), a display of the standard line (100 ms), and finally a screen with a blue fixation dot, signaling subjects to report their response. The subject pressed a key on a numeric keypad with the index or ring finger of his or her right hand to indicate that he or she perceived the comparison line or the standard line, respectively, to be longer. Response time was not limited. No feedback was provided.

Conditions and sessions

We chose the orientations of the standard and comparison lines independently from the eight possible values for a total of 64 orientation conditions. Each session contained 10 trials in each orientation condition for a total of 640 trials per session in pseudorandom order. Each subject completed five sessions, together containing 50 trials in each of the 64 orientation conditions for a total of 3,200 trials.

Instructions and practice

At the start of the first session, we explained the task to the subject. Specifically, we mentioned that the second line in each trial would always have the same length, that each line would vary in orientation from trial to trial, and that the experiment was only about judging length, not orientation. At the start of each subsequent session, we checked for understanding by

asking the subjects what they had to report, which of the two lines would always have the same length, and whether they had to pay attention to orientation. In the first session, subjects completed eight practice trials right after the instructions; we did not analyze these trials.

Stimulus selection

In the first trial within each of the 64 orientation conditions, we chose the length of the comparison line randomly from the 61 possible values. In every subsequent trial in a given condition (across the entire experiment), we chose the length of the comparison line using Luigi Acerbi’s MATLAB implementation (<https://github.com/lacerbi/psybayes>) of the Ψ method by Kontsevich and Tyler (1999), extended to include the lapse rate (Prins, 2012). This algorithm maintained, separately for each orientation condition, a joint posterior distribution over the point of subjective equality (PSE; between 2 and 4 cm in 51 steps), the logarithm of the noise parameter [between $\log(0.05 \text{ cm})$ and $\log(1.5 \text{ cm})$ in 25 steps], and the lapse rate (between 0 and 0.2 in 25 steps) of the psychometric curve in that condition. After each subject response, the algorithm updated this posterior and returned the length of the comparison line for the next trial to maximize the expected information gain. Specifically, we minimized the entropy of the distribution after the next trial, averaged over the two possible responses and weighted by the probability of those responses under the current posterior. We used the following priors:

- For the PSE, a discretized normal distribution with a mean of 3 cm and a standard deviation of 2 cm.
- For the logarithm of the noise parameter, a uniform distribution across the possible values; this corresponds to a Jeffreys’ prior, which has the desirable property of being invariant under reparameterizations.
- For the lapse rate, a beta distribution with parameters 1 and 24. This prior is monotonically decreasing, so favors low lapse rates.

The exact form of these priors is not very important: First, they will quickly get overridden by the evidence from the subject responses; second, the proof of stimulus selection is in the pudding, and we show below that the chosen stimuli suffice for accurate estimation of psychometric curve parameters.

Psychometric curve fitting

The fitting of the psychometric curves is complicated by the fact that we assume a single lapse rate across all

64 orientation conditions. In a given trial in the i th condition, we assume that the probability of reporting that the comparison line was longer takes the form (Wichmann & Hill, 2001)

$$p(\text{report "comparison longer"}|s, \mu_i, \sigma_i, \lambda) = \frac{\lambda}{2} + (1 - \lambda)\Phi(s; \mu_i, \sigma_i), \quad (1)$$

where s is the length of the comparison line on that trial, μ_i is the PSE in the i th condition, σ_i is the noise parameter in the i th condition, and λ is the lapse rate. We assume that the lapse rate is shared across all conditions. For each individual subject, we estimated the 64 values of μ , the 64 values of σ , and λ using posterior mean estimation.

We will need the log likelihood function in each individual condition, denoted by LL_i ; this function is defined as

$$LL_i(\mu_i, \sigma_i, \lambda) = \log p(\text{data}_i | \mu_i, \sigma_i, \lambda) = \sum_{j=1}^{50} \log p(\text{report}_j | s_j, \mu_i, \sigma_i, \lambda), \quad (2)$$

where i is the condition index, j is the trial index within the condition, report_j is the subject's report ("comparison longer" or "standard longer") on the j th trial, s_j is the comparison length on the j th trial, and $p(\text{report}_j | s_j, \mu_i, \sigma_i, \lambda)$ is given by Equation 1.

The posteriors over the parameters can now be expressed in terms of the log likelihood function (for the derivation, see Appendix A):

$$p(\lambda | \text{data}) = \frac{\prod_{k=1}^{64} \iint e^{LL_k(\mu_k, \sigma_k, \lambda)} d\mu_k d\sigma_k}{\int \left(\prod_{k=1}^{64} \iint e^{LL_k(\mu_k, \sigma_k, \lambda)} d\mu_k d\sigma_k \right) d\lambda} \quad (3)$$

$$p(\mu_i | \text{data}, \lambda) = \frac{\int e^{LL_i(\mu_i, \sigma_i, \lambda)} d\sigma_i}{\iint e^{LL_i(\mu_i, \sigma_i, \lambda)} d\mu_i d\sigma_i}$$

$$p(\sigma_i | \text{data}, \lambda) = \frac{\int e^{LL_i(\mu_i, \sigma_i, \lambda)} d\mu_i}{\iint e^{LL_i(\mu_i, \sigma_i, \lambda)} d\mu_i d\sigma_i}$$

Finally, we obtain Bayesian least-squares estimates of all parameters by taking the means of their posteriors:

$$\hat{\lambda} = \int \lambda p(\lambda | \text{data}) d\lambda$$

$$\hat{\mu}_i = \int \mu_i p(\mu_i | \text{data}) d\mu_i \quad (4)$$

$$\hat{\sigma}_i = \int \sigma_i p(\sigma_i | \text{data}) d\sigma_i$$

We evaluated all integrals through Riemann integration using linear grids over μ_i (between 2 and 4 cm in 51

steps), σ_i (between 0.05 cm and 1.5 cm in 25 steps), and λ (between 0 and 0.2 in 25 steps).

Results

Psychometric curves

Using a two-interval, forced choice paradigm, we studied how perceived length depends on orientation for isolated stimuli. We controlled visual field using an eye patch and a circular aperture. Standard and comparison lines could each take one of eight orientations for a total of 64 orientation conditions. Because the data were collected using an adaptive method, plotting the raw data would result in clusters of points that are not helpful in conveying the underlying pattern. Therefore, we show only the fits to the data (Figure 2). For each condition, we show both the mean fit (solid lines) and the standard error of the fit across subjects (shaded regions). Visual inspection indicates that in all conditions, the psychometric curve for a vertical comparison line lies to the left of the psychometric curve for a horizontal comparison line, meaning that the vertical line is perceived as longer.

We estimated PSEs, noise parameters, and lapse rates of the psychometric curves using Bayesian least-squares estimation (see Methods and Appendix A). The Bayesian posterior distributions in Equation 3 not only produce the point estimates in Equation 4, but also uncertainty levels. Averaged across all 64 conditions, the posterior standard deviation of the PSE was 0.083 ± 0.011 cm (here and elsewhere: mean \pm standard error of the mean), indicating that 50 trials per condition and the adaptive Bayesian method produced rather certain estimates.

Figure 3A shows the estimated PSE as a function of the orientation of the comparison line for different orientations of the standard line. This demonstrates the HVI: To make a horizontal line appear equally long as a nonhorizontal line, it has to be longer. A two-way ANOVA revealed a significant main effect of comparison orientation on PSE, $F(7, 56) = 18.43$, $p < 10^{-11}$; a significant main effect of standard orientation, $F(7, 56) = 13.18$, $p < 10^{-9}$; and no significant interaction, $F(49, 392) = 1.21$, $p = 0.17$.

Examining the noise parameter σ of the psychometric curves, we did not find a significant effect of comparison orientation, $F(7, 56) = 1.30$, $p = 0.27$; a significant effect of standard orientation, $F(7, 56) = 1.36$, $p = 0.24$; or a significant interaction, $F(49, 392) = 1.28$, $p = 0.11$ (see Figure A2). This suggests that length was not encoded with substantially greater precision at some orientations than at others.

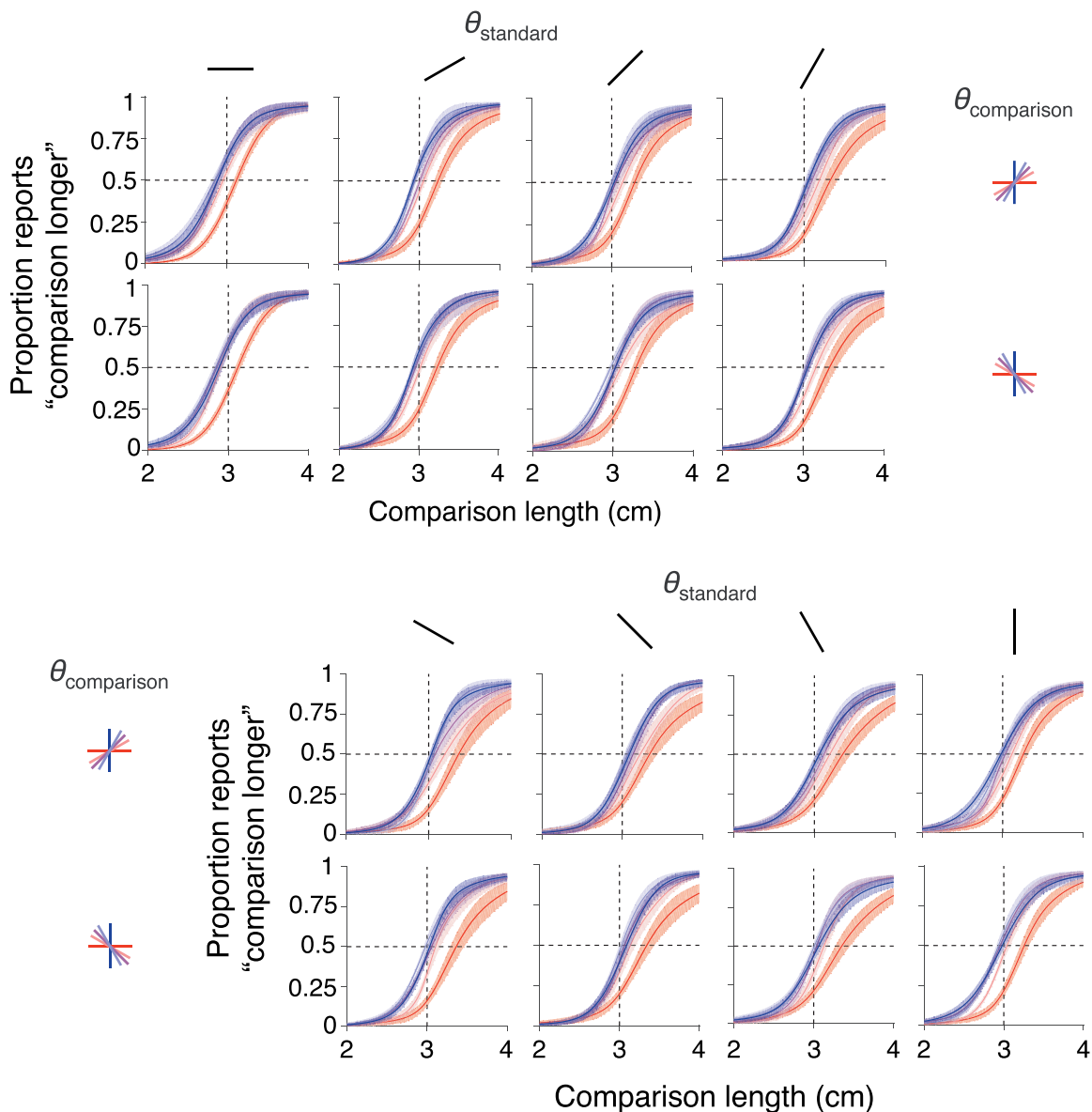


Figure 2. Fitted psychometric curves. Each curve shows the fit of a cumulative Gaussian distribution with a lapse rate to the proportion of trials in which the comparison line was reported to appear longer as a function of the length of the comparison line. We fitted the data per subject but show the mean across subjects (solid lines) and ± 1 SEM (shaded areas). Across plots, the orientation of the standard line differed as indicated by the black icons: In the first two rows, the orientation of the standard line was (from left to right) 0° , 30° , 45° , or 60° ; in the bottom two rows, it was 150° , 135° , 120° , or 90° . Within each plot, each color corresponds to an orientation of the comparison line as indicated by the colored icons: In the first and third rows, these orientations were 0° , 30° , 45° , 60° , or 90° ; in the second and fourth rows, they were 90° , 120° , 135° , 150° , or 0° . The psychometric curve for a 0° comparison line (red curves) is consistently to the right of the psychometric curve for a 90° comparison line (blue curve), which means vertical lines were perceived as longer than horizontal lines.

Bias toward second interval

Selecting only the conditions in which $\theta_{\text{comparison}} = \theta_{\text{standard}}$, we obtained Figure 3B. This shows a clear bias toward reporting the standard line (the line in the second interval) as longer. For each subject, we defined the *interval bias ratio* (IBR) as the average PSE across all conditions with $\theta_{\text{comparison}} = \theta_{\text{standard}}$, divided by the

length of the standard. The mean IBR estimated in this way was 1.0224 ± 0.0088 , or $2.24\% \pm 0.88\%$ larger than 1.

Multiplicative bias model

Next, we were interested in the ratios of perceived lengths at different orientations. To infer those, we

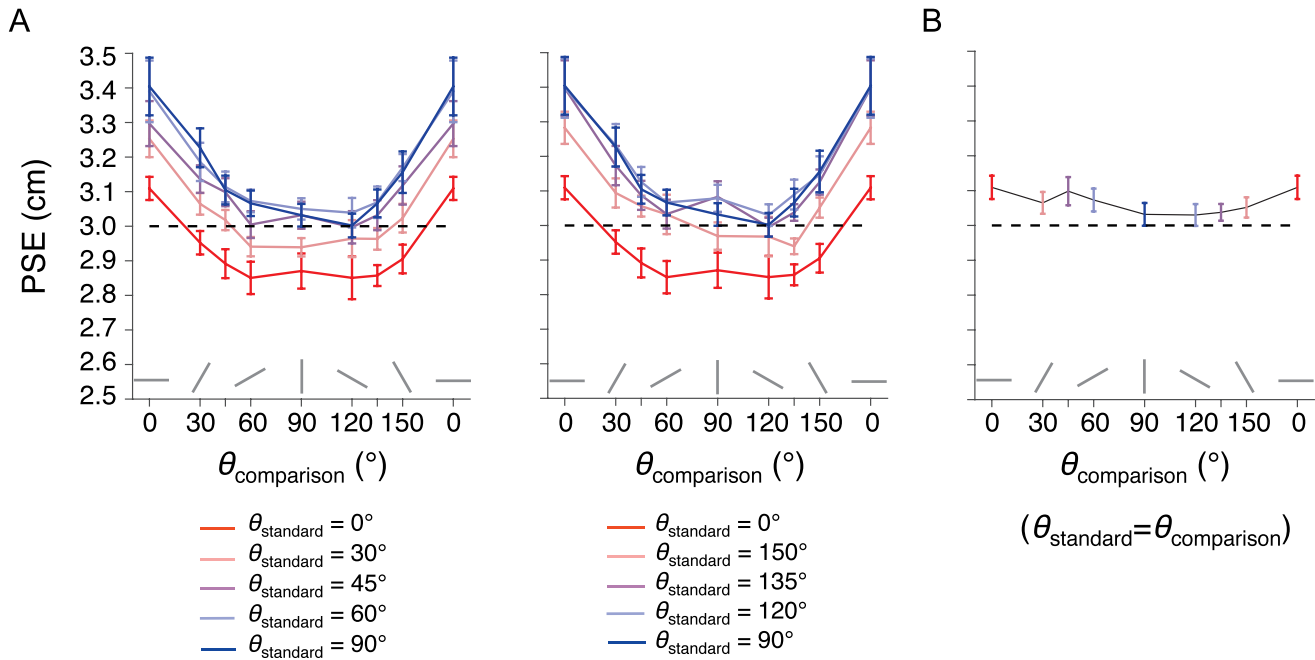


Figure 3. (A) Mean and standard error of the mean of the estimated PSE as a function of the orientation of the comparison line for different orientations of the standard line (divided over two plots for visibility). The black dashed line represents the length of the standard line (3 cm, dashed line). On each curve, the PSE of a nonhorizontal comparison line is lower than that of a horizontal comparison line (U shape); in other words, a nonhorizontal comparison line does not need to be as long as a horizontal comparison line to be perceived as equally long. Looking across curves, a comparison line of a given orientation needs to be longer to be perceived as equally long as a nonhorizontal standard line than as a horizontal standard line. (B) Mean and standard error of the mean of the estimated PSE for equal θ_{standard} and $\theta_{\text{comparison}}$. These data are a subset of the data in panel A. Subjects had an overall bias for reporting that the standard line (in the second interval) was longer.

have to express the measured PSEs in terms of perceived lengths. We use a descriptive model in which the average perceived length $\langle \hat{L} \rangle$ of a line of orientation θ equals the true length L multiplied by an orientation-dependent bias factor $OB(\theta)$ as well as by an interval-dependent bias factor $IB(\text{interval})$:

$$\langle \hat{L} \rangle = IB(\text{interval})OB(\theta)L.$$

The PSE is the true length L of the comparison for which the average perceived length is equal to the average perceived length of the standard. Thus,

$$\begin{aligned} \langle \hat{L}_{\text{comparison}} \rangle &= \langle \hat{L}_{\text{standard}} \rangle OB(\theta_{\text{comparison}}) \cdot \text{PSE} \\ &= \frac{IB(\text{second interval})}{IB(\text{first interval})} \cdot OB(\theta_{\text{standard}}) \cdot L_{\text{standard}}, \end{aligned} \quad (5)$$

where $L_{\text{standard}} = 3$ cm. It follows that

$$\text{PSE} = \frac{IB(\text{second interval})}{IB(\text{first interval})} \cdot \frac{OB(\theta_{\text{standard}})}{OB(\theta_{\text{comparison}})} \cdot L_{\text{standard}}. \quad (6)$$

By applying the definition of IBR from the previous

subsection, we find $IBR = [IB(\text{second interval})] / [IB(\text{first interval})]$. Both $\theta_{\text{comparison}}$ and θ_{standard} take eight possible values, giving rise to 64 PSE values. To fit this descriptive model, we minimized the sum of the squares of the differences between the empirical PSEs and the ones described by Equation 6:

$$\text{Minimize} \sum_{i=1}^{64} \left(\text{PSE}_i - \frac{OB(\theta_{\text{standard},i})}{OB(\theta_{\text{comparison},i})} \cdot IBR \cdot L_{\text{standard}} \right)^2.$$

Because this objective function is invariant to a common scaling of all OBs, we define the *normalized orientation-dependent bias* as $OB^*(\theta) = [OB(\theta)] / [OB(\theta = 0^\circ)]$, so that the objective function becomes

$$\sum_{i=1}^{64} \left(\text{PSE}_i - \frac{OB^*(\theta_{\text{standard},i})}{OB^*(\theta_{\text{comparison},i})} \cdot IBR \cdot L_{\text{standard}} \right)^2.$$

We then minimized this objective function over the eight parameters: IBR, $OB^*(30^\circ)$, $OB^*(45^\circ)$, ..., $OB^*(150^\circ)$, excluding $OB^*(0^\circ)$, which by definition equals 1. We implemented the minimization, for each individual subject, using *fmincon* in Matlab with 100 random initializations.

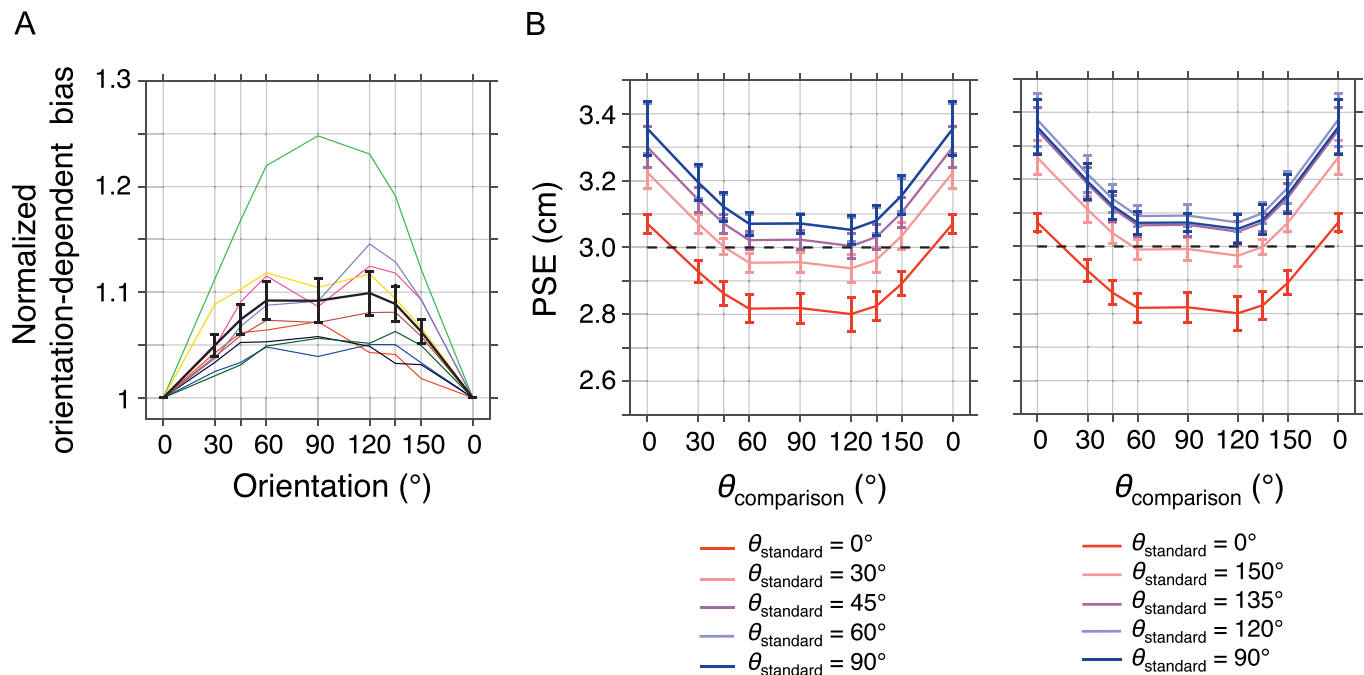


Figure 4. Multiplicative bias model. (A) Estimated normalized orientation-dependent bias as a function of orientation, estimated from the multiplicative bias model. Colors: individual subjects. Black: mean and standard error of the mean. (B) Fitted PSE values according to the multiplicative bias model. The model closely accounts for the empirical PSEs in Figure 3A.

This minimization yielded a mean estimated IBR of 1.0238 ± 0.0094 —in line with the estimates obtained from only the $\theta_{\text{comparison}} = \theta_{\text{standard}}$ conditions (reported in the previous subsection). Next, Figure 4 and Table 1 show the estimated normalized orientation-dependent bias. The orientation-dependent bias tends to be stronger for orientations closer to vertical. Signed-rank tests did not reveal significant differences between the normalized orientation-dependent biases at 30° and 150° ($z = 1.24$, $p = 0.21$), between the ones at 45° and 135° ($z = 1.71$, $p = 0.09$), or between the ones at 60° and 120° ($z = 1.13$, $p = 0.26$). Thus, we did not find any evidence for asymmetry around vertical.

Orientation	Normalized orientation-dependent bias, OB \times (mean \pm standard error of the mean)
0° (horizontal)	1 (by definition)
30°	1.050 ± 0.010
45°	1.074 ± 0.014
60°	1.092 ± 0.018
90° (vertical)	1.092 ± 0.021
120°	1.099 ± 0.021
135°	1.089 ± 0.017
150°	1.063 ± 0.011

Table 1. Normalized orientation-dependent bias as a function of orientation.

Comparison with earlier work

In terms of the HVI in the narrow sense, our estimated normalized vertical bias of $9.2\% \pm 2.1\%$ is in reasonable agreement with some previous studies, which found, for example, 8.3% and 8.7% (Pollock & Chapanis, 1952), 7.1% (Künnapas, 1957b), $11.5\% \pm 1.4\%$ (Craven, 1993), and 9.3% and 8.9% (Armstrong & Marks, 1997), but substantially larger than in others, such as 2.6% (Avery & Day, 1969), 4.0% (Künnapas, 1957a), and 6% (Mamassian & de Montalembert, 2010).

More interestingly, we can compare our results to those of other studies of the HVI that varied orientation: Pollock and Chapanis (1952), Cormack and Cormack (1974), and Craven (1993). In all cases, we are interested in the *orientation-dependent bias ratio* $[\text{OB}(\theta_{\text{standard}})] / [\text{OB}(\theta_{\text{comparison}})]$, which in our data is equal to $\text{PSE} / (\text{IBR} \times L_{\text{standard}})$, according to Equation 6. Comparison with these papers is complicated by two factors. First, we varied the orientations of both the standard and the comparison lines, and the earlier studies always fixed the orientation of one of them. Therefore, in the following analyses, we selected the corresponding subset of our trials. Second, the earlier studies used different metrics than we did to report the illusion; we map all metrics to ours, namely $[\text{OB}(\theta_{\text{standard}})] / [\text{OB}(\theta_{\text{comparison}})]$. We now review the details of the three studies.

Pollock and Chapanis (1952) used an adjustment task in which subjects viewed a horizontal or vertical standard line of length 3 in. (7.62 cm) or 6 in. (15.24 cm) and adjusted a comparison line of variable orientation to match the standard line in length. Standard and comparison lines were presented side by side with a separation of 9 in. in the 3-in. condition or a separation of 18 in. in the 6-in. condition. Twenty subjects each performed two judgments in each condition. The authors reported the mean and standard deviation of “error,” the difference between the length of the comparison and the length of the standard. In terms of our variables, this is

$$\begin{aligned} \text{Error} &\equiv L_{\text{comparison}} - L_{\text{standard}} \\ &= \left(\frac{\text{OB}(\theta_{\text{standard}})}{\text{OB}(\theta_{\text{comparison}})} - 1 \right) L_{\text{standard}}. \end{aligned}$$

In order to compare their data with ours, we computed mean and standard error of the mean of $(\text{Error} / L_{\text{standard}}) + 1$ based on the data given in table I of Pollock and Chapanis (1952) (this table only gives standard deviations, so we divided those values by $\sqrt{40}$, which is the total number of judgments in each condition).

Craven (1993) used a two-alternative forced-choice task in which subjects simultaneously viewed a horizontal standard line of length 50 arcmin of visual angle (1.45 cm at their viewing distance) and a nonhorizontal comparison length. Standard and comparison were spatially separated in both the x and y dimensions. Subjects reported whether the left or the right line appeared longer. The author reported mean and standard error of the mean of the apparent length of the nonhorizontal line with respect to the horizontal length; because the author used an additive model, we interpret this quantity as

$$\frac{L_{\text{standard}} - (\text{PSE} - L_{\text{standard}})}{L_{\text{standard}}} = 2 - \frac{\text{PSE}}{L_{\text{standard}}}.$$

Cormack and Cormack (1974) used an adjustment task in which subjects viewed a nonhorizontal standard line of length 10 cm. Subjects adjusted a horizontal comparison line to match the perceived length of the standard. Standard and comparison formed a configuration; here, we only select their experiments in which the configuration was left/right symmetric. In “cross-like” configurations, the midpoints of standard and comparison coincided; in “inverted T-like” configurations, the lower end of the standard line was the midpoint of the comparison line. The authors reported mean and standard error of the mean of the “illusion magnitude,” which is the same as error above but with a different L_{standard} (10 cm).

We extracted data from the first panel of figure 1 of Cormack and Cormack (1974) and from figure 1 of

Study	R^2 with our study (Figure 5)
Pollock and Chapanis (1952) 3-in. horizontal standard	0.64
Pollock and Chapanis 6-in. horizontal standard	0.68
Pollock and Chapanis 3-in. vertical standard	0.60
Pollock and Chapanis 6-in. vertical standard	0.73
Craven (1993)	0.80
Cormack and Cormack (1974) cross-like configuration	−0.10
Cormack and Cormack inverted T-like configuration	0.92

Table 2. Correspondence between earlier studies and ours. Notes: We use R^2 as a measure of similarity. Because this is not linear regression, R^2 can be negative, and the value of -0.10 is not a mistake.

Craven (1993) using the free, web-based data-extraction software WebPlotDigitizer (Rohatgi, 2016); we obtained the Pollock & Chapanis (1952) data from their table 1. For our data, we estimated the orientation-dependent bias ratios using the appropriate subset of trials and individual-subject IBR estimates. Figure 5 shows the resulting comparison. The correspondence is qualitatively good. To quantify the similarity, we made pairwise comparisons of the means between our study and each earlier study. Because the orientations used were not identical between any pair of studies, we interpolated both ways between the y values using the piecewise cubic hermite interpolating polynomial algorithm (*interp1* with “pchip” in Matlab). We did not allow for extrapolation, i.e., we limited the orientations to the narrower range between the two studies. We then evaluated goodness of fit by R^2 on the interpolated means:

$$R^2 = 1 - \frac{\text{var}(\text{mean_study1} - \text{mean_study2})}{\frac{\text{var}(\text{mean_study1}) + \text{var}(\text{mean_study2})}{2}}.$$

The resulting values are shown in Table 2.

The only poor correspondence is between our study and the cross-like (“+”) configuration in Cormack and Cormack (1974). This is due to an irregular point at vertical in their curve: The vertical line was perceived as *shorter* than lines at orientations of 45° , 67.5° , 112.5° , and 135° . This is an effect that was emphasized by later authors (Craven, 1993; Howe & Purves, 2002). By contrast, in our data, signed-rank tests did not reveal significant differences between the normalized orientation-dependent biases at 60° and 90° ($z = 0.18$, $p = 0.86$), between the ones at 90° and 120° ($z = 0.77$, $p = 0.44$), or between the ones at 90° and 135° ($z = 0.059$, $p = 0.95$); a signed-rank test *did* reveal a significant difference between the normalized bias factors at 45° and 90° ($z = 2.43$, $p = 0.015$) but in the direction opposite to Cormack and Cormack. We have no good explanation for this discrepancy, but we suspect that it is due to a special property of the “+” configuration.

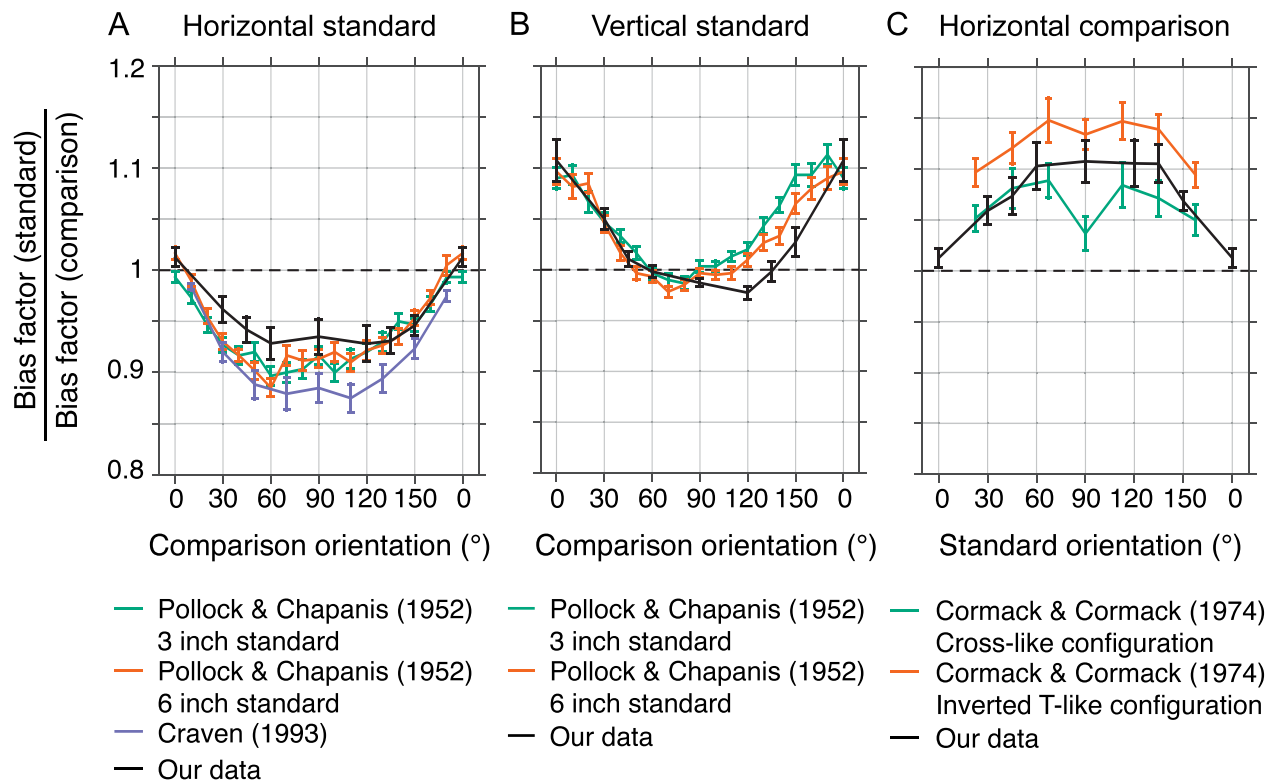


Figure 5. Comparison with earlier work. Comparison of the estimated orientation-dependent bias ratios (standard to comparison, estimated from the multiplicative bias model) between our data (without configuration) and earlier studies (with configuration). (A) Conditions in which the standard line (fixed length) was horizontal. (B) Conditions in which the standard line was vertical. (C) Conditions in which the comparison line (variable length) was horizontal.

Anisotropy model

The multiplicative bias model describes the measured PSEs but does not explain the origin of orientation-dependent length biases. If the observer is rational, such biases would result from statistical inference under ambiguity. The ambiguity consists of the fact that a given retinal length could have been produced by infinitely many possible physical lengths. The rational way to resolve this ambiguity would be to determine which physical length is most probable for a given retinal length. Length biases would then be orientation-dependent if the retinal orientation and the retinal length of a line segment are correlated for a given physical length. Howe and Purves (2002) measured this correlation by using a laser range scanner to record the 3-D locations of points in a natural scene, then randomly sampling pairs of points in the projected image and obtaining the mean ratio of physical length to projected length as a function of projected orientation (Figure 7B). They found that this mean ratio was higher for nonhorizontal projected orientations than for horizontal and highest at projected orientations of about 60° and 120°. For line segments associated with luminance contrast boundaries, the data were noisier

than for pairs of points but showed qualitatively the same pattern although of a much larger magnitude. Howe and Purves proceeded to hypothesize that the orientation dependence of the mean ratio of physical to projected length is in large part due to the presence of the ground plane in most natural scenes: In this plane, lines that extend more in depth have projections that tend toward vertical and, at the same time, are foreshortened to a greater extent. Indeed, they found that when the ground plane was left out, the orientation dependence of the mean ratio was much reduced.

Here, we extend these ideas by providing an explicit geometric model of the projection of 3-D orientations onto a plane and performing simulations to determine the effect of particular types of anisotropy in three dimensions. We refer to this as the *anisotropy model*. We constrain this model by using not only the Howe and Purves (2002) data, but also the distribution of projected orientations in natural scenes.

Geometry

We first need to express the projected orientation and length of a line in terms of that line's physical orientation and length in 3-D space. We sketched the

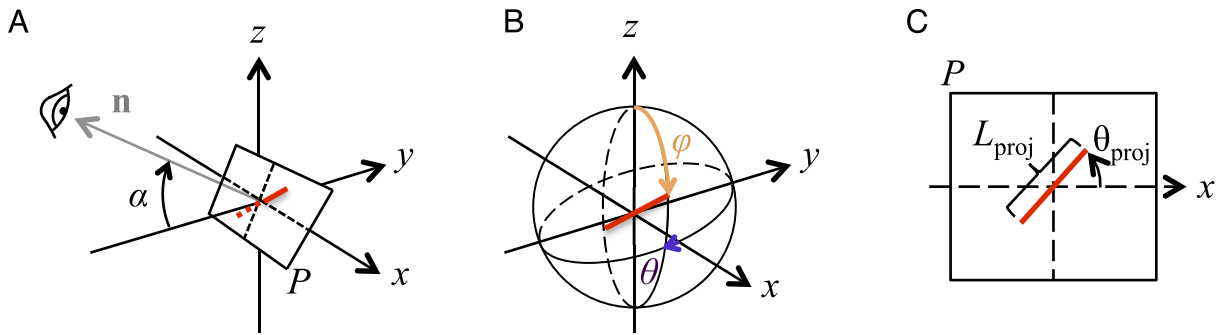


Figure 6. Anisotropy model. (A) Three-dimensional geometry of line length perception. A line segment (red) has its midpoint at the origin. P is the frontoparallel plane through the origin, and \mathbf{n} is the normal vector to the plane. α is the viewing angle. (B) Spherical coordinates of one end of the line segment. θ is the azimuth, φ the polar angle. (C) Projected length L_{proj} and projected angle θ_{proj} of the line segment.

relevant geometry in Figure 6. We consider a line segment of half length L whose midpoint is the origin of a 3-D Cartesian coordinate system. The line segment has spherical coordinates θ (azimuth, with $\theta = 0$ corresponding to the x -axis) and φ (polar angle, with $\varphi = 0$ corresponding to a vertical line). This means that one of its end points has Cartesian coordinates $\mathbf{v} = L(\cos\theta \sin\varphi, \sin\theta \sin\varphi, \cos\varphi)$, and the other the negative of this. An observer’s eye is located on the $x = 0$ plane and views the origin at an angle α ; in other words, the eye’s coordinates are $\mathbf{n} = (0, -\cos\alpha, \sin\alpha)$. We define a projection plane P through the origin, orthogonal to the observer’s line of sight (i.e., a frontoparallel plane); in other words, \mathbf{n} is the unit normal vector of P . The projection of the line segment onto P will be a scaled version of the projection of the line segment onto the observer’s retina, provided that we can reasonably approximate the retina as locally flat (this is reasonable when the observer is not too close to the line segment). Because we are interested in length bias ratios, the scale factor is irrelevant.

Expressions for projected length and projected orientation

We are now ready to derive expressions for projected length and projected orientation. Thus, our goal is to map properties of the vector \mathbf{v} to properties of its projection onto the plane P , \mathbf{v}_{proj} :

$$\left. \begin{array}{l} \text{3D Vector } \mathbf{v} \\ \text{Half – length : } L \\ \text{Polar angle } \varphi \\ \text{Azimuth } \theta \text{ (uniformly distributed)} \\ \text{Projection plane } P \\ \text{Normal } \mathbf{n} = (0, -\cos\alpha, \sin\alpha) \end{array} \right\} \rightarrow \left\{ \begin{array}{l} \text{Projected vector } \mathbf{v}_{\text{proj}} \\ \text{Projected half – length } L_{\text{proj}} \\ \text{Projected orientation } \theta_{\text{proj}} \end{array} \right. \quad (7)$$

The projection of \mathbf{v} onto P is $\mathbf{v} - (\mathbf{v} \cdot \mathbf{n})\mathbf{n}$, where \cdot is the inner product. We work this out in our case:

$$\begin{aligned} \mathbf{v}_{\text{proj}} &= \mathbf{v} - (\mathbf{v} \cdot \mathbf{n})\mathbf{n} \\ &= L \begin{bmatrix} \cos\theta \sin\varphi \\ \sin\theta \sin\varphi \\ \cos\varphi \end{bmatrix} - L(-\sin\theta \sin\varphi \cos\alpha + \cos\varphi \sin\alpha) \begin{bmatrix} 0 \\ -\cos\alpha \\ \sin\alpha \end{bmatrix} \\ &= L \begin{bmatrix} \cos\theta \sin\varphi \\ \sin\theta \sin\varphi \sin^2\alpha + \cos\varphi \cos\alpha \sin\alpha \\ \sin\theta \sin\varphi \sin\alpha \cos\alpha + \cos\varphi + \cos^2\alpha \end{bmatrix}. \end{aligned}$$

The length of this projected vector can be evaluated as

$$\begin{aligned} L_{\text{proj}} &= \|\mathbf{v}_{\text{proj}}\| \\ &= L\sqrt{\cos^2\theta \sin^2\varphi + (\sin\theta \sin\varphi \sin\alpha + \cos\varphi \cos\alpha)^2}. \end{aligned}$$

We define the “foreshortening factor” (FF) as the ratio between the projected length and the physical length:

$$\begin{aligned} \text{FF}(\theta, \varphi, \alpha) &= \frac{L_{\text{proj}}}{L} \\ &= \sqrt{\cos^2\theta \sin^2\varphi + (\sin\theta \sin\varphi \sin\alpha + \cos\varphi \cos\alpha)^2}. \quad (8) \end{aligned}$$

The projected orientation θ_{proj} is defined within the projection plane P as the angle between \mathbf{v}_{proj} and the x -axis (which lies in P). The cosine of this angle is

$$\cos\theta_{\text{proj}} = \frac{\mathbf{v}_{\text{proj}} \cdot \begin{bmatrix} 1 \\ 0 \\ 0 \end{bmatrix}}{\|\mathbf{v}_{\text{proj}}\|} = \frac{L \cos\theta \sin\varphi}{L_{\text{proj}}} = \frac{\cos\theta \sin\varphi}{\text{FF}(\theta, \varphi, \alpha)}.$$

This can be simplified using the tangent:

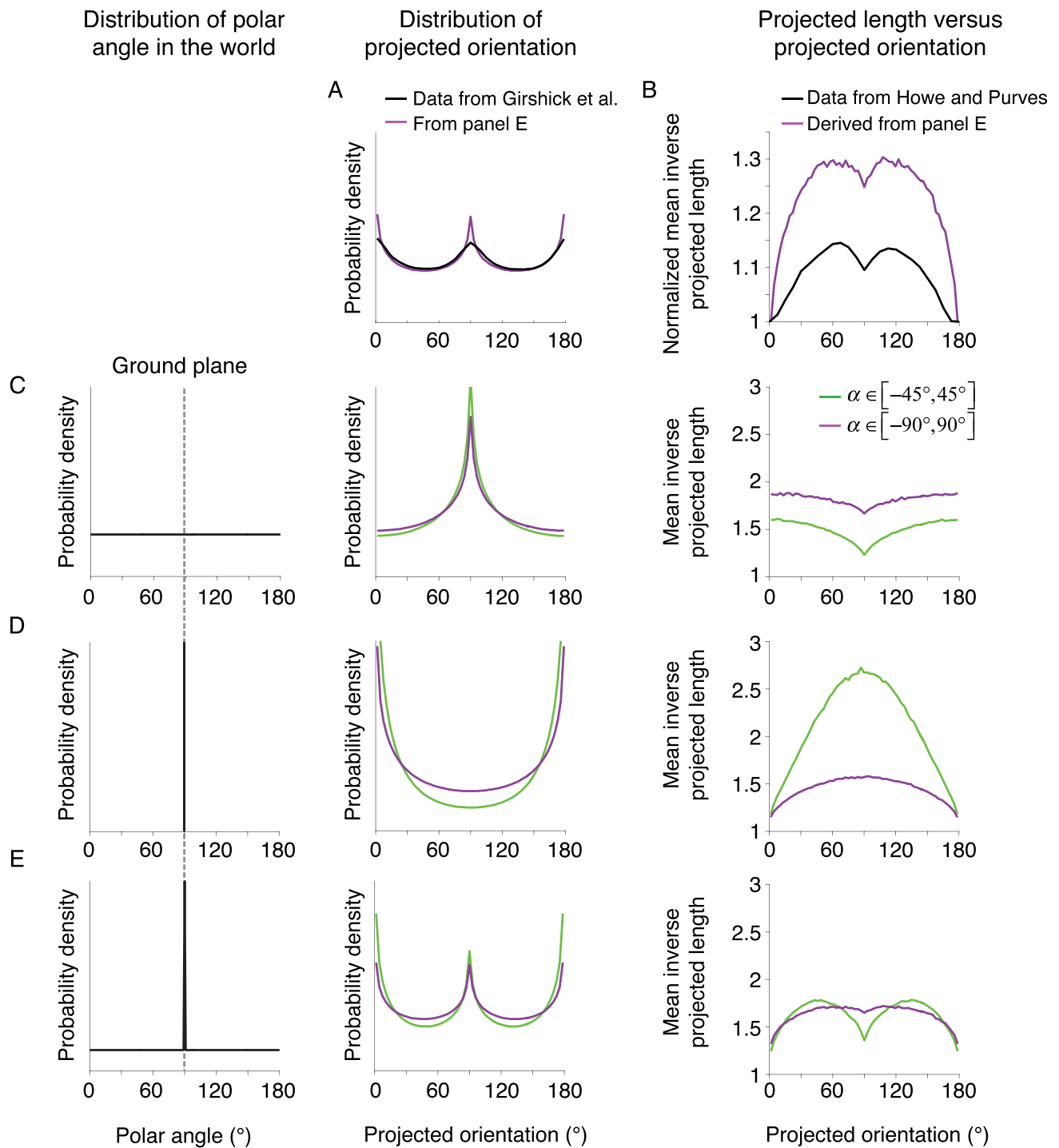


Figure 7. The anisotropy model can simultaneously account for the distribution of projected orientation and for orientation-dependent length biases. (A) Distribution of projected orientation: natural statistics from Girshick et al. (2011) (black) and anisotropy model (purple). (B) Normalized mean ratio of physical length to projected length: natural statistics from Howe and Purves (2002) (black) and anisotropy model. (C) When polar angle is uniformly distributed (isotropic orientation, left), the model matches neither the distribution of projected orientation (center) nor the relationship between projected length and projected orientation (right). (D) When all lines are in the ground plane (polar angle of 90°), the model reproduces the HVI but not the distribution of projected orientation. (E) Mixture model: To obtain approximately equal prevalence of horizontal and vertical projected orientations (center), a polar angle of 90° needs to be much more common than all others (left).

$$\tan \theta_{\text{proj}} = \sqrt{\frac{1}{\cos^2 \theta_{\text{proj}}} - 1} = \tan \theta \sin \alpha + \frac{\cos \alpha}{\cos \theta \tan \varphi}.$$

Two special cases provide useful sanity checks:

- If $\alpha = \pi/2$, the observer has a top view. Then, $\text{FF} = \sin \varphi$ and $\theta_{\text{proj}} = \theta$.
- If $\varphi = 0$, the line is vertical. Then, $\text{FF} = \cos \alpha$ and $\theta_{\text{proj}} = \pi/2$ (also vertical).

In view of the shared dependences on θ , φ , and α , projected length L_{proj} and projected orientation θ_{proj} will not be independent.

The distributions of projected length and projected orientation

For an observer in a real-world environment, the polar angle φ , the azimuth θ , and the viewing angle α will not be constant but will obey a probability distribution $p(\theta, \varphi, \alpha)$. For a given true length, projected length and projected orientation will inherit their distribution from this distribution through the mapping in Equation 7. Formally,

$$\begin{aligned} p(L_{\text{proj}}, \theta_{\text{proj}} | L) &= \iiint p(L_{\text{proj}}, \theta_{\text{proj}} | L, \theta, \varphi, \alpha) p(\theta, \varphi, \alpha) d\theta d\varphi d\alpha \\ &= \iiint p(\theta_{\text{proj}} | L_{\text{proj}}, \theta, \varphi) p(L_{\text{proj}} | L, \theta, \varphi, \alpha) \\ &\quad \cdot p(\theta, \varphi, \alpha) d\theta d\varphi d\alpha \\ &= \iiint \delta\left(\theta_{\text{proj}} - \arccos \frac{\cos \theta \sin \varphi}{\text{FF}(\theta, \varphi, \alpha)}\right) \\ &\quad \times \delta(L_{\text{proj}} - L \cdot \text{FF}(\theta, \varphi, \alpha)) \\ &\quad \times p(\theta, \varphi, \alpha) d\theta d\varphi d\alpha \end{aligned}$$

Some data from natural scenes are available to constrain this joint distribution over L_{proj} and θ_{proj} . First, to obtain a marginal distribution over projected orientation, $p(\theta_{\text{proj}})$, Girshick, Landy, and Simoncelli (2011) extracted orientations from photographs of natural scenes (for a predecessor of this work, see Coppola, Purves, McCoy, & Purves, 1998). The data show that a projected orientation is more often horizontal or vertical than oblique (Figure 7A). Second, regarding the conditional distribution $p(L_{\text{proj}} | \theta_{\text{proj}}, L)$, which captures the relationship between projected length and projected orientation, we use the aforementioned data from Howe and Purves (2002) (Figure 7B).

Simulations

The idea of the anisotropy model is that we can account for $p(L_{\text{proj}}, \theta_{\text{proj}} | L)$ and, in particular, for the

summary statistics in Figure 7A and B, by suitably choosing the distribution $p(\theta, \varphi, \alpha)$. Without loss of generality, we set $L = 1$. To further constrain the problem, we assume that θ , φ , and α are independent so that their joint distribution factorizes: $p(\theta, \varphi, \alpha) = p(\theta)p(\varphi)p(\alpha)$. We also assume that azimuth θ is uniformly distributed between 0 and 2π ; it seems strange to assume anything else. Then, anisotropy can only result from $p(\varphi)$ or $p(\alpha)$ not being uniform. For simplicity, we choose $p(\alpha)$ to be uniform either on the interval $[-45^\circ, 45^\circ]$ (and 0 outside it) or on $[-90^\circ, 90^\circ]$.

We performed three sets of simulations, each with a different choice of $p(\varphi)$. In each simulation, we randomly drew θ , φ , and α from their respective distributions and computed the histogram of projected orientations as well as the mean of the inverse of projected length for different projected orientation bins. The mean of the inverse of projected length corresponds to the mean of the ratio of physical to projected length that Howe and Purves (2002) use because our physical length equals one.

In Simulation 1, we assumed that $p(\varphi)$ is uniform (Figure 7C, left), which means that the distribution of line orientation in 3-D space is *isotropic*. Nevertheless, the distribution of projected orientation is not uniform at all but has a strong peak at vertical (Figure 7C, center). The projected length is *greater* for vertical than for horizontal (Figure 7C, right), which contradicts the HVI. This suggests that, in the absence of true correlations between length and orientation in the world, anisotropy is needed to explain the HVI.

In Simulation 2 (Figure 7D, left), we consider an extremely anisotropic distribution, in which all lines lie in the horizontal plane (the ground plane); in other words, $z = 0$ or $\varphi = \pi/2$. Then, the foreshortening factor is $\sqrt{1 - \sin^2 \theta \cos^2 \alpha}$, and the tangent of the projected angle is $\tan \theta_{\text{proj}} = \tan \theta \sin \alpha$. This predicts that projected orientation is much more often horizontal than any other orientation without vertical being special (Figure 7D, center). It also predicts that the projected length is smaller for projected orientations closer to vertical (Figure 7D, right) as already noted by Howe and Purves (2002). Both effects are qualitatively more consistent with the data, in particular with the HVI, than Simulation 1.

In Simulation 3, we used a mixture of the uniform distribution from Simulation 1 and the delta function from Simulation 2. We chose the mixture proportion of the delta function to be 0.45. This would correspond to a world in which a large proportion of lines lie in the ground plane, and other polar angles are equally represented. The resulting distribution of θ_{proj} (Figure 7E, center) is qualitatively similar to the distribution of projected orientations reported by Girshick et al. (2011) (Figure 7A). As we might expect from Simulation 1, a polar angle of $\pi/2$ (horizontal) needs to be *much more*

frequent than a polar angle of 0 or π (vertical) for a projected orientation of horizontal to be about as frequent as a projected orientation of vertical. Furthermore, when $p(\alpha)$ is uniform on $[-\pi/2, \pi/2]$, these choices produce a pattern of projected length as a function of orientation that is consistent with the HVI (Figure 7E, right). To compare with the data from Howe and Purves (2002) (Figure 7B), we normalized the mean inverse projected length by dividing by its value in the bin that includes horizontal ($\theta_{\text{proj}} = 0^\circ$); this yields a curve similar to the data (Figure 7B). The magnitude of the effect is off, but the empirical data are also equivocal on the magnitude because, for contours, the mean ratio might be much higher than the data in Figure 7B (Howe & Purves, 2002). We conclude that a high prevalence of ground plane lines with a broad distribution of other polar angles can qualitatively account for both the empirical distribution of orientation on the retina and for the empirical relationship between retinal length and retinal orientation.

Relationship to behavior

So far, we have only explored the distribution of orientations and lengths that the retina inherits from the 3-D world; in other words, we have described a “forward model” or “generative model” of retinal orientations and lengths. We have not yet described how the observer would utilize these statistics when doing our task. Such a description is naturally provided by Bayesian decision theory. In a Bayesian explanation, the observer would regard an image of a line segment viewed during the experiment as a photograph of a line segment in 3-D space. The observables are then projected length L_{proj} and projected orientation θ_{proj} whereas the length of the 3-D line segment L , its angles θ and φ , and the viewing angle of the camera α , are not observable. The generative model would be specified by the conditional distribution $p(L_{\text{proj}}, \theta_{\text{proj}} | L)$. The observer would infer L from L_{proj} and θ_{proj} while marginalizing over θ , φ , and α . In this inference, $p(L_{\text{proj}}, \theta_{\text{proj}} | L)$ would serve as the likelihood function over L . The likelihood functions over L from the first and second intervals would be used to make the decision. If, for a given projected orientation θ_{proj} , the FF L_{proj}/L tends to be lower, the observer will be biased to judge the line at that projected orientation as longer to “compensate for” the foreshortening. Thus, the observer would infer that a vertical line ($\theta_{\text{proj}} = 90^\circ$) was longer than a horizontal line ($\theta_{\text{proj}} = 0$) of the same retinal length. Thus, in a Bayesian view, the distribution $p(L_{\text{proj}} | \theta_{\text{proj}}, L)$ would be the basis for orientation-dependent length biases. The Bayesian strategy would not be optimal with respect to the laboratory statistics; it would have been optimal if the laboratory had been the real world.

Based on Figure 7B, this inference model is qualitatively consistent with one aspect of our behavioral data—nonhorizontal lines are judged as longer than horizontal lines—but not with another; our subjects did not show a dip in perceived length at vertical orientations. It should be kept in mind that a full-fledged inference model goes beyond Figure 7B because that figure only shows the mean of the ratio L/L_{proj} , not the distribution $p(L_{\text{proj}} | \theta_{\text{proj}}, L)$. Given how many poorly justified assumptions we already had to make to match the data in Figure 7A and B, there is little point in trying to work out the inference process in detail. Instead, we view the anisotropy model as a proof of concept that anisotropy in polar angle might account for orientation-dependent length biases.

Effect of slant: A critique of Hibbard, Goutcher, O’Kane, and Scarfe (2012)

Although not fully worked out, the anisotropy model is Bayesian in the same vein as the model proposed by Howe and Purves (2002). Hibbard et al. (2012) criticized those authors’ Bayesian explanation of the HVI based on an experiment using virtual slanted surfaces. They provided binocular and texture cues about slant, and the subject had to adjust the image aspect ratio to make a slanted ellipse appear circular (Figure 8A). They reasoned that the HVI results from overestimating the slant of a frontoparallel surface based on a prior favoring highly slanted surfaces (i.e., with the top farther away than the bottom). They attempted to nullify the effect of this prior by providing a negative slant measurement (i.e., one with the top closer than the bottom). The idea was that for some value of this measurement, the posterior over slant would be centered near frontoparallel, and the HVI should disappear. Instead, they found that the HVI persisted, leading them to reject the Bayesian framework. They concluded by describing the subject’s reported image aspect ratio as a function of slant using a cosine function, acknowledging that this was heuristic rather than principled.

Their argument might be based on a faulty assumption about the prior distribution over slant. Hibbard et al. (2012) modeled the prior over slant as a Gaussian distribution (Figure 8A). By contrast, in the anisotropy model, it is far from Gaussian. To see this, first consider the prior over polar angle (Figure 7E), which consists of a peak at 90° for the ground plane and a uniform distribution elsewhere. Restricted to $\theta = \pm 90^\circ$ (the plane formed by the observer’s line of sight and the ground plane normal), this translates to the prior over slant depicted in Figure 8B (solid line), which has peaks at $\pm 90^\circ$ and a uniform distribution elsewhere. Multiplying this prior by the likelihood

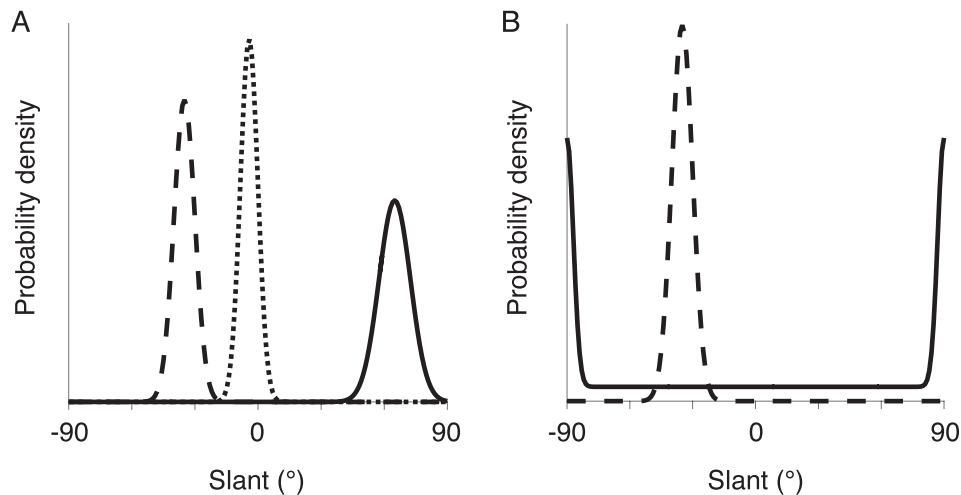


Figure 8. The anisotropy model applied to slanted surfaces. (A) Solid: prior distribution over slant assumed by Hibbard et al. (2012). Dashed: example likelihood over slant based on a slant cue. Dotted: the posterior peaks in between the likelihood and the prior. (B) Solid: prior distribution over slant corresponding to the prior over polar angle from Figure 7E (with the peaks at -90° and 90° widened slightly for visibility). Dashed: same likelihood as in panel A. The posterior over slant will be nearly identical to the likelihood.

corresponding to the negative slant cue yields a posterior distribution that is nearly identical to the likelihood: This is because the region of high prior density corresponds to low likelihood, thereby removing the effect of the prior. Even if the peaks in the prior density are wider, the posterior shifts toward $\pm 90^\circ$ rather than toward 0° . In either case, the observer is predicted to set lower aspect ratios for surfaces slanted away from frontoparallel in either direction. In the extreme case that the slant cue provides perfect information about slant, we can simply apply Equation 8 with $\theta = \pm 90^\circ$ to find that $FF = |\cos(\varphi \alpha)|$, which has exactly the same cosine form as advocated by Hibbard et al. Thus, Hibbard et al.'s rejection of a Bayesian account might be premature.

Discussion

Using a two-interval design with a circular visual field and Bayesian adaptive stimulus selection, we studied the HVI in the absence of configuration effects. We varied the orientations of both the standard and the comparison line in a full factorial design. First, we reproduced the illusion. Second, specific to the two-interval design, we found an overall bias toward reporting that the standard line (in the second interval) was longer; we estimated the corresponding bias to be 1.0224 ± 0.0088 using the PSEs from the conditions in which standard and comparison had the same orientation and as 1.0238 ± 0.0094 from a multiplicative bias model applied to all conditions. Third, using that same model, we found a

gradual, sine-like increase of the normalized orientation-dependent bias going from horizontal to vertical with an estimated value of 1.092 ± 0.021 at vertical. Fourth, also when correcting for the interval bias, we found that the orientation-dependent length biases in our data were quantitatively similar to those reported in three earlier studies. Fifth, we developed a model in which a simple anisotropy in the polar angle of line segments in three dimensions, after projection, accounts for both the observed distribution of projected orientations and for the observed relationship between projected length and projected orientation; the latter, combined with Bayesian inference, might account for orientation-dependent length biases. The model predicts that a polar angle of 90° (corresponding to the ground plane) is much more common than any other polar angle. Sixth, the model also reconciles Hibbard et al.'s (2012) results for slanted surfaces with a Bayesian account.

Interval biases have been found in many previous studies, but depending on different factors, such as interval length, stimulus magnitude, and distractors, in either direction (Ashourian & Loewenstein, 2011; v. G. T. Fechner, 1860; Fraise, 1948; Hellström, 1985; Hollingworth, 1910; Needham, 1935; Vierordt, 1868; Woodrow, 1933; Yeshurun, Carrasco, & Maloney, 2008). Theories proposed for these biases include a “persistence” of the first stimulus (G. T. Fechner, 1882; v. G. T. Fechner, 1860), a central tendency (Hollingworth, 1910), and a Bayesian prior (Ashourian & Loewenstein, 2011). Our study cannot distinguish between these theories. Moreover, in our design, we cannot rule out that the fact the standard line was always in the second interval played a role.

More work is needed to establish whether orientation-dependent length biases are Bayesian. First, the distribution of the polar angle of lines in natural environments and the distribution of observer viewing angle in natural viewing need to be characterized. Second, the effect of sensory noise needs to be incorporated in the model. If a Bayesian account holds, then the question arises what determines to what extent observers in psychophysical experiments use priors derived from natural statistics versus priors derived from the experimental stimulus distributions. More specifically for the HVI, why would people bring to bear statistics from 3-D scenes on the inference of stimuli that quite obviously lie in a frontoparallel plane?

Keywords: horizontal–vertical illusion, length perception, Bayesian observer, natural statistics

Acknowledgments

Commercial relationships: none.
Corresponding author: Wei Ji Ma.
Email: weijima@nyu.edu.
Address: Center for Neural Science and Department of Psychology, New York University.

References

- Armstrong, L., & Marks, L. E. (1997). Differential effects of stimulus context on perceived length: Implications for the horizontal-vertical illusion. *Perception and Psychophysics*, *59*(8), 1200–1213.
- Ashourian, P., & Loewenstein, Y. (2011). Bayesian inference underlies the contraction bias in delayed comparison tasks. *PLoS One*, *6*(5), e19551.
- Avery, G. C., & Day, R. H. (1969). Basis of the horizontal-vertical illusion. *Journal of Experimental Psychology*, *81*(2), 376–380.
- Brainard, D. H. (1997). The Psychophysics Toolbox. *Spatial Vision*, *10*(4), 433–436.
- Brosvic, G. M., & Cohen, B. D. (1988). The horizontal-vertical illusion and knowledge of results. *Perceptual and Motor Skills*, *67*(2), 463–469.
- Coppola, D. M., Purves, H. R., McCoy, A. N., & Purves, D. (1998). The distribution of oriented contours in the real world. *Proceedings of the National Academy of Sciences, USA*, *95*(7), 4002–4006.
- Cormack, E. O., & Cormack, R. H. (1974). Stimulus configuration and line orientation in the horizontal-vertical illusion. *Perception & Psychophysics*, *16*(2), 208–212.
- Craven, B. J. (1993). Orientation dependence of human line-length judgements matches statistical structure in real-world scenes. *Proceedings of the Royal Society of London B: Biological Sciences*, *253*(1336), 101–106.
- Fechner, G. T. (1882). *Revision der Hauptpunkte der Psychophysik* [Translation: *Revision of the main points of psychophysics*]. Leipzig: Breitkopf & Härtel.
- Fechner, G. T. (1860). *Elemente der Psychophysik* [Translation: *Elements of psychophysics*]. Leipzig: Breitkopf & Härtel.
- Fick, A. (1851). *Tractatus de errore quodam optico asymmetria bulbi oculi effecto* [Treatment on a certain optical error caused by asymmetry of the eyeball]. Marburg (dissertation).
- Finger, F. W., & Spelt, D. K. (1947). The illustration of the horizontal-vertical illusion. *Journal of Experimental Psychology*, *37*(3), 243–250.
- Fraisse, P. (1948). Les erreurs constantes dans la reproduction de courts intervalles temporels [Translation: Constant errors in the reproduction of short time intervals]. *Archives de Psychologie*, *32*, 161–176.
- Gentaz, E., & Hatwell, Y. (2004). Geometrical haptic illusions: The role of exploration in the Muller-Lyer, vertical-horizontal, and Delboeuf illusions. *Psychonomics Bulletin and Review*, *11*(1), 31–40.
- Girgus, J. S., & Coren, S. (1975). Depth cues and constancy scaling in the horizontal-vertical illusion: The bisection error. *Canadian Journal of Psychology*, *29*(1), 59–65.
- Girshick, A. R., Landy, M. S., & Simoncelli, E. P. (2011). Cardinal rules: Visual orientation perception reflects knowledge of environmental statistics. *Nature Neuroscience*, *14*(7), 926–932.
- Gregory, R. L. (1974). *Concepts and mechanisms of perception*. London: Duckworth.
- Hamburger, K., & Hansen, T. (2010). Analysis of individual variations in the classical horizontal-vertical illusion. *Attention, Perception, and Psychophysics*, *72*(4), 1045–1052.
- Heller, M. A., Calcaterra, J. A., Burson, L. L., & Green, S. L. (1997). The tactual horizontal-vertical illusion depends on radial motion of the entire arm. *Perception and Psychophysics*, *59*(8), 1297–1311.
- Heller, M. A., & Joyner, T. D. (1993). Mechanisms in the haptic horizontal-vertical illusion: Evidence

- from sighted and blind subjects. *Perception and Psychophysics*, 53(4), 422–428.
- Hellström, Å. (1985). The time-order error and its relatives: Mirrors of cognitive processes in comparing. *Psychological Bulletin*, 97(1), 35–61.
- Hibbard, P. B., Goutcher, R., O’Kane, L. M., & Scarfe, P. (2012). Misperception of aspect ratio in binocularly viewed surfaces. *Vision Research*, 70, 34–43.
- Higashiyama, A. (1996). Horizontal and vertical distance perception: The discorded-orientation theory. *Perception and Psychophysics*, 58(2), 259–270.
- Hollingworth, H. L. (1910). The central tendency of judgment. *The Journal of Philosophy, Psychology and Scientific Methods*, 7(17), 461–469.
- Howe, C. Q., & Purves, D. (2002). Range image statistics can explain the anomalous perception of length. *Proceedings of the National Academy of Sciences, USA*, 99(20), 13184–13188.
- Jackson, R. E., & Cormack, L. K. (2008). Evolved navigation theory and the environmental vertical illusion. *Evolution and Human Behavior*, 29(5), 299–304.
- Jahoda, G., & Stacey, B. (1970). Susceptibility to geometrical illusions according to culture and professional training. *Perception & Psychophysics*, 7(3), 179–184.
- Klein, B. J., Li, Z., & Durgin, F. H. (2016). Large perceptual distortions of locomotor action space occur in ground-based coordinates: Angular expansion and the large-scale horizontal-vertical illusion. *Journal of Experimental Psychology: Human Perception and Performance*, 42(4), 581–593.
- Kontsevich, L. L., & Tyler, C. W. (1999). Bayesian adaptive estimation of psychometric slope and threshold. *Vision Research*, 39(16), 2729–2737.
- Künnapas, T. M. (1955). An analysis of the “vertical-horizontal illusion.” *Journal of Experimental Psychology*, 49(2), 134.
- Künnapas, T. M. (1957a). Interocular differences in the vertical-horizontal illusion. *Acta Psychologica*, 13, 253–259.
- Künnapas, T. M. (1957b). The vertical-horizontal illusion and the visual field. *Journal of Experimental Psychology*, 53(6), 405–407.
- Künnapas, T. M. (1959). The vertical-horizontal illusion in artificial visual fields. *The Journal of Psychology*, 47(1), 41–48.
- Lipshits, M., McIntyre, J., Zaoui, M., Gurfinkel, V., & Berthoz, A. (2001). Does gravity play an essential role in the asymmetrical visual perception of vertical and horizontal line length? *Acta Astronautica*, 49(3), 123–130.
- Mamassian, P., & de Montalembert, M. (2010). A simple model of the vertical-horizontal illusion. *Vision Research*, 50(10), 956–962.
- Michaels, R. M. (1960). Anisotropy and interaction of fields of spatial induction. *Journal of Experimental Psychology*, 60(4), 235–241.
- Needham, J. G. (1935). The effect of the time interval upon the time-error at different intensive levels. *Journal of Experimental Psychology*, 18(5), 530–543.
- Pearce, D., & Matin, L. (1969). Variation of the magnitude of the horizontal-vertical illusion with retinal eccentricity. *Perception & Psychophysics*, 6(4), 241–243.
- Pelli, D. G. (1997). The VideoToolbox software for visual psychophysics: Transforming numbers into movies. *Spatial Vision*, 10, 437–442.
- Pollock, W. T., & Chapanis, A. (1952). The apparent length of a line as a function of its inclination. *Quarterly Journal of Experimental Psychology*, 4(4), 170–178.
- Prins, N. (2012). The psychometric function: The lapse rate revisited. *Journal of Vision*, 12(6):25, 1–16, doi:10.1167/12.6.25. [PubMed] [Article]
- Prinzmetal, W., & Gettleman, L. (1993). Vertical-horizontal illusion: One eye is better than two. *Perception & Psychophysics*, 53(1), 81–88.
- Rohatgi, A. (2016). WebPlotDigitizer 3.10. Available at <http://arohatgi.info/WebPlotDigitizer>
- Schiffman, H. R., & Thompson, J. G. (1975). The role of figure orientation and apparent depth in the perception of the horizontal-vertical illusion. *Perception*, 4(1), 79–83.
- Segall, M. H., Campbell, D. T., & Herskovits, M. J. (1963). Cultural differences in the perception of geometric illusions. *Science*, 139(3556), 769–771.
- Teghtsoonian, M. (1972). Apparent length as a function of tilt does not depend on orientation of the standard. *Journal of Experimental Psychology*, 94(2), 191–197.
- Vierordt, K. (1868). *Der Zeitsinn nach Versuchen* [Translation: *The time-sense according to experiments*]. Tübingen: Laupp.
- Von Collani, G. (1985). The horizontal-vertical illusion in photographs of concrete scenes with and without depth information. *Perceptual and Motor Skills*, 61(2), 523–531.
- Wichmann, F. A., & Hill, N. J. (2001). The psychometric function: I. Fitting, sampling, and

goodness of fit. *Perception and Psychophysics*, 63(8), 1293–1313.

Williams, P. A., & Enns, J. T. (1996). Pictorial depth and framing have independent effects on the horizontal-vertical illusion. *Perception*, 25, 921–926.

Wolfe, U., Maloney, L. T., & Tam, M. (2005). Distortions of perceived length in the frontoparallel plane: Tests of perspective theories. *Perception and Psychophysics*, 67(6), 967–979.

Woodrow, H. (1933). Weight-discrimination with a varying standard. *The American Journal of Psychology*, 45(3), 391–416.

Wundt, W. M. (1862). *Beiträge zur Theorie der Sinneswahrnehmung* [Translation: *Contribution to the theory of sensory perception*]. Leipzig: W. Engelmann.

Yeshurun, Y., Carrasco, M., & Maloney, L. T. (2008). Bias and sensitivity in two-interval forced choice procedures: Tests of the difference model. *Vision Research*, 48(17), 1837–1851.

Appendix A: Fitting multiple psychometric curves with a shared lapse rate

In an experiment with multiple conditions, it often happens that one or more parameters are shared among conditions. An example is a lapse rate, which is usually regarded as the probability that the subject blinks or has a lapse of attention; there is often no strong reason to believe that the lapse rate will vary across experimental conditions. Assuming that a parameter is shared across conditions will allow for more precise estimation of the remaining parameters. Below and in Figure A1, we describe the posterior distributions and posterior mean estimates of the parameters in such situations. This treatment is not tied to our specific experiment.

Step 1: Parameter log likelihood by condition. We index condition by i . We assume we have a parameter log likelihood by condition—in our cases, $LL_i(\mu_i, \sigma_i, \lambda)$ as given by Equation 2. Here, λ represents the parameter(s) that is (are) shared among conditions whereas μ_i and σ_i are both condition-specific parameters. We denote the set of all μ_i 's collectively by $\vec{\mu}$ and the set of all σ_i 's by $\vec{\sigma}$.

Step 2: Posterior over shared parameter. It turns out to be easiest to first compute the posterior over λ . We

do this by marginalizing over the μ 's and σ 's and assuming uniform priors over all variables:

$$\begin{aligned} p(\lambda|\text{data}) &\propto p(\text{data}|\lambda) \\ &= \iint p(\text{data}|\vec{\mu}, \vec{\sigma}, \lambda) d\vec{\mu} d\vec{\sigma} \\ &= \iint \left(\prod_k p(\text{data}_k|\mu_k, \sigma_k, \lambda) \right) d\vec{\mu} d\vec{\sigma} \\ &= \prod_k \iint p(\text{data}_k|\mu_k, \sigma_k, \lambda) d\mu_k d\sigma_k \\ &= e^{\sum_k LL_k^*} \prod_k \iint e^{LL_k(\mu_k, \sigma_k, \lambda) - LL_k^*} d\mu_k d\sigma_k \\ &\propto \prod_k \iint e^{LL_k(\mu_k, \sigma_k, \lambda) - LL_k^*} d\mu_k d\sigma_k \quad (9) \end{aligned}$$

where LL_k^* is the maximum log likelihood across parameter combinations in the k th condition. We separated this term off to prevent the exponentials inside the integrals from being numerically zero. Normalizing, we find for the posterior over λ ,

$$p(\lambda|\text{data}) = \frac{\prod_k \iint e^{LL_k(\mu_k, \sigma_k, \lambda) - LL_k^*} d\mu_k d\sigma_k}{\int \left(\prod_k \iint e^{LL_k(\mu_k, \sigma_k, \lambda) - LL_k^*} d\mu_k d\sigma_k \right) d\lambda}$$

Step 3: Posterior over a condition-specific parameter given λ . We now compute the posterior over μ_i conditioned on λ . This is easy because λ is the only variable that connects the conditions; therefore, when λ is given, the posterior over μ_i only depends on the data in the i th condition:

$$\begin{aligned} p(\mu_i|\text{data}, \lambda) &= p(\mu_i|\text{data}_i, \lambda) \propto p(\text{data}_i|\mu_i, \lambda) \\ &= \int p(\text{data}_i|\mu_i, \sigma_i, \lambda) d\sigma_i \\ &= \int e^{LL_i(\mu_i, \sigma_i, \lambda)} d\sigma_i. \end{aligned}$$

Normalizing, we find

$$p(\mu_i|\text{data}, \lambda) = \frac{\int e^{LL_i(\mu_i, \sigma_i, \lambda)} d\sigma_i}{\iint e^{LL_i(\mu_i, \sigma_i, \lambda)} d\mu_i d\sigma_i} \quad (10)$$

Similarly, the posterior of the noise parameter in the i th condition, σ_i , conditioned on λ is

$$p(\sigma_i|\text{data}, \lambda) = \frac{\int e^{LL_i(\mu_i, \sigma_i, \lambda)} d\mu_i}{\iint e^{LL_i(\mu_i, \sigma_i, \lambda)} d\mu_i d\sigma_i} \quad (11)$$

Step 4: Posterior over a condition-specific parameter. Now we are ready to compute the posterior over μ_i not conditioned on λ by integrating over the conditioned posterior:

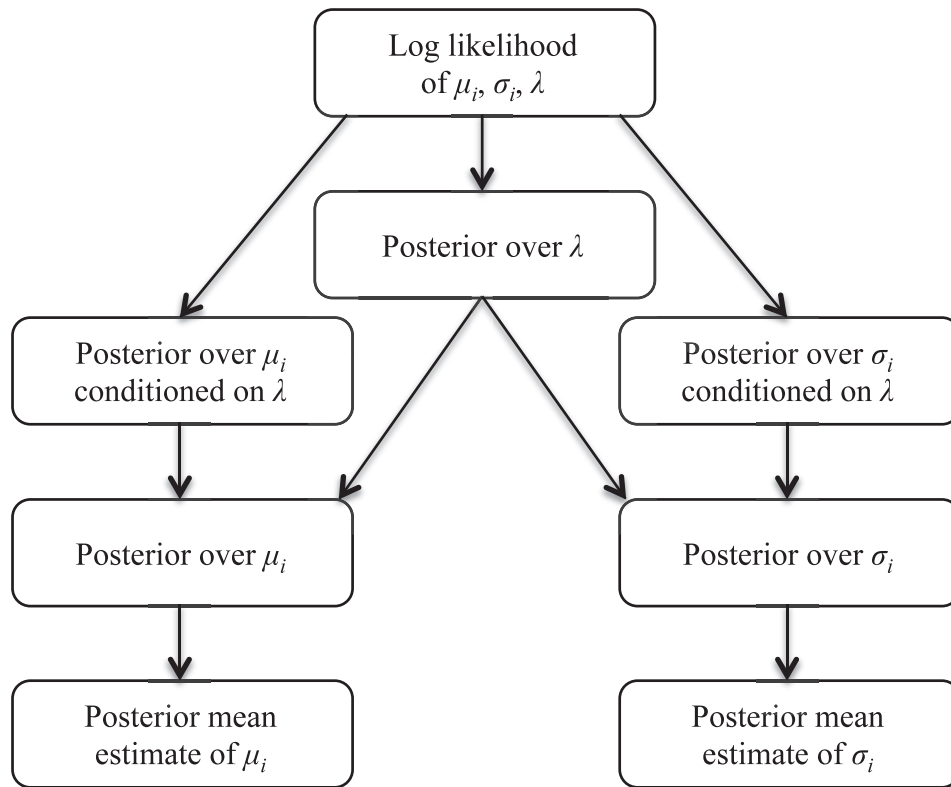


Figure A1. Flow diagram for Bayesian estimation of the psychometric curve parameters μ_i and σ_i when multiple conditions are assumed to share the same lapse rate λ .

$$p(\mu_i|\text{data}) = \int p(\mu_i|\text{data}, \lambda)p(\lambda|\text{data}) d\lambda, \quad (12)$$

where the first factor in the integrand is given by Equation 10 and the second factor by Equation 9.

Similarly, the posterior of σ_i , is given by

$$p(\sigma_i|\text{data}) = \int p(\sigma_i|\text{data}, \lambda)p(\lambda|\text{data}) d\lambda. \quad (13)$$

Finally, we can obtain point estimates by taking the means under these posteriors.

Appendix B: Estimates of the noise parameters of the psychometric curves

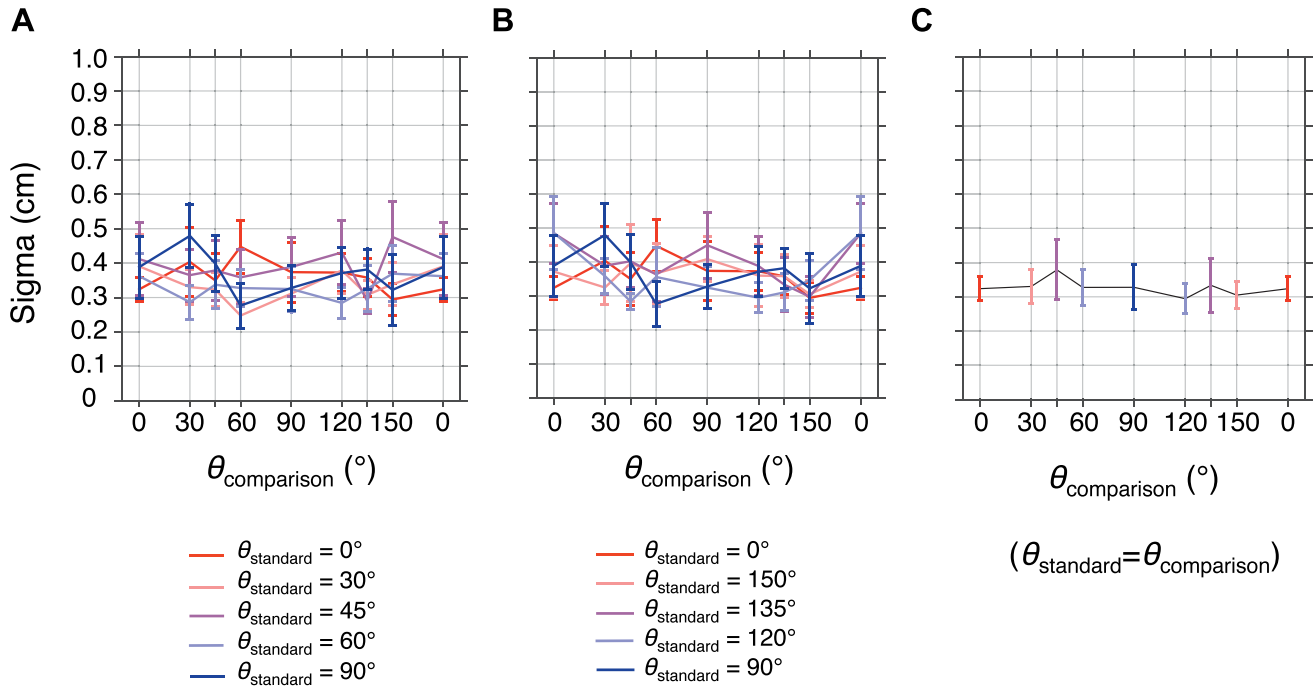


Figure A2. Mean and standard error of the mean of the estimate of the noise parameter σ_i of the psychometric curve as a function of the orientation of the comparison line when the orientation of the standard line was (A) 0° , 30° , 45° , 60° , or 90° or (B) 90° , 120° , 135° , 150° , or 0° . (C) Mean and standard error of the mean of the estimate of σ_i when θ_{standard} equals $\theta_{\text{comparison}}$. These data are a subset of the data in panels A and B.